

Entropic estimate of cooperative binding of substrate on a single oligomeric enzyme: An index of cooperativity

Kinshuk Banerjee, Biswajit Das and Gautam Gangopadhyay^{1, a)}

S.N.Bose National Centre For Basic Sciences

Block-JD, Sector-III, Salt Lake, Kolkata-700098, India.

Here we have systematically studied the cooperative binding of substrate molecules on the active sites of a single oligomeric enzyme in a chemiostatic condition. The average number of bound substrate and the net velocity of the enzyme catalyzed reaction are studied by the formulation of stochastic master equation for the cooperative binding classified here as spatial and temporal. We have estimated the entropy production for the cooperative binding schemes based on single trajectory analysis using a kinetic Monte Carlo technique. It is found that the total as well as the medium entropy production show the same generic diagnostic signature for detecting the cooperativity, usually characterized in terms of the net velocity of the reaction. This feature is also found to be valid for the total entropy production rate at the nonequilibrium steady state. We have introduced an index of cooperativity, C , defined in terms of the ratio of the surprisals or equivalently, the stochastic system entropy associated with the fully bound state of the cooperative and non-cooperative cases. The criteria of cooperativity in terms of C is compared with that of the Hill coefficient and gives a microscopic insight on the cooperative binding of substrate on a single oligomeric enzyme which is usually characterized by macroscopic reaction rate.

Keywords: Oligomeric enzyme kinetics, Cooperativity, Stochastic thermodynamics, Single trajectory

^{a)}Electronic mail: gautam@bose.res.in

I. INTRODUCTION

Conventional thermodynamics at or near equilibrium needs serious modification to accommodate the events of single molecular processes as well as nano-systems which are generally in states far away from equilibrium¹⁻¹⁰. The single molecule study is very important in biological systems because most of the processes in cell are taking place on the level of a single or a few molecules. The non-equilibrium feature is mainly developed within a cell due to the mechanical or chemical stimuli which runs the metabolism through the driven chemical reactions^{11,12}. Quantitative measure of fluctuations¹³⁻²⁰ in small systems are possible over short periods of time that allow the thermodynamic concepts to be applied to such finite systems. A crucial concept in the statistical description of a nonequilibrium small system is that of a single trajectory or path^{9,13,16,19} and defining the entropy of the system for such a single trajectory allows one to formulate the second law of thermodynamics at the stochastic level²¹⁻²⁴. The trajectory-based entropy production²¹⁻²³ has been successfully applied to various systems, for example, single bio-molecular reactions¹¹, chemical reaction networks²² and driven colloidal particles²³.

Enzyme kinetics is a very important process in cellular metabolism where nonequilibrium feature is developed due to the imbalanced chemical reactions and the presence of chemiostatic condition prevents the reaction system to attain equilibrium²⁵⁻²⁸. In a chemiostatic condition, substrate and product are maintained at constant concentrations by continuous influx of the substrate and withdrawing the product from the system. Under this condition, the reaction system reaches a nonequilibrium steady state (NESS)²⁵⁻²⁷ which is characterized by a non-zero total entropy production rate. Single molecule enzyme kinetics^{29,30} is theoretically studied using the stochastic master equation approach^{31,32} as well as by the stochastic single trajectory analysis^{11,12}. Now most of the enzymes found in enzymology are oligomeric in nature consisting of two or more subunits usually linked to each other by non-covalent interactions³³. Possibility of interaction between the subunits during the substrate binding process can give rise to different cooperative phenomena³³⁻³⁶. Positive cooperativity is said to occur when the binding of one substrate molecule with a subunit increases the affinity of further attachment of the substrate to another subunit^{33,34,37}. In the case of negative cooperativity, attachment of a substrate molecule to one subunit decreases the tendency of further attachment of the substrate molecules to other

subunits^{38,39}. These types of cooperativity based on the affinity of the substrate binding belong to the class of allosteric cooperativity^{34–37}. There is another type of cooperativity, termed as temporal cooperativity⁴⁰, reflected in the zero-order ultra sensitivity of the phosphorylation-dephosphorylation cycle which is shown to be mathematically equivalent to the allosteric cooperativity³¹. Beside allosterism, cooperativity has been studied in monomeric enzymes with only a single substrate binding site. This has led to the important concept of hysteretic^{32,34,41} and mnemonic enzymes^{42,43}. These two types of enzymes show the cooperativity phenomena due to the slow conformational disorder of the active site³².

In this paper, we have studied the entropy production in the kinetics of a single oligomeric enzyme which shows cooperativity with respect to the substrate binding. Here we have classified the cooperativity phenomena according to the nature of the different substrate binding mechanisms, namely, sequential and independent, as detailed by Weiss⁴⁴. In sequential binding, the adjacent sites of the oligomeric enzyme are successively occupied by the substrate molecules. So the substrate-bound states of the system are actually adjacent in space and hence we denote the cooperativity arising out of this binding protocol as the spatial cooperativity. For the sequential mechanism, the first binding site, *i.e.*, the first subunit of the oligomeric enzyme must be filled in order for the second site to become occupied by the substrate, as if the substrate molecules have been stacked on top of each other at their binding sites⁴⁴. This type of binding can be relevant to an ion transporter, such as the Na-K pump⁴⁵. The other class is called temporal cooperativity which can occur due to the independent binding of the substrate molecules to any one of the subunits at a particular time without any specific spatial arrangement. Here the substrate-bound sites are not physically neighboring in the enzyme⁴⁰ but the global state of the system is defined in terms of the total occupancy of the overall sites at a particular instant of time. This type of binding can be observed in multimeric proteins with individual binding sites located on different subunits, such as ligand gated ion channels or ligand gated enzymes⁴⁴. Here we have theoretically studied the cooperative behavior solely from the viewpoint of the substrate binding mechanism and not in terms of the active and inactive enzyme conformations or the actual structural details of the enzyme that can lead to such mechanisms^{46,47}. To study the bulk kinetics of allosteric enzymes Monod, Wyman and Changeux (MWC) in 1965 and Koshland, Nemethy and Filmer (KNF) in 1966 put forward models to account for cooperative binding. Generally ‘Sequential’ is used as a term for a classical distinction between multi-step bind-

ing models, as for instance differentiating between the KNF and MWC models in terms of the variation of the substrate binding rates in each successive step. So the term sequential in KNF model should not be confused with the term sequential used in our approach^{44,48}. We have constructed the master equations for each class of substrate binding. Time evolution of such cooperative systems can be described by suitably applying a kinetic Monte Carlo technique^{49,50}. Here we have applied this algorithm to calculate the total, medium and system entropy production along a single trajectory for such cooperative systems as a function of the substrate concentration over a time interval where finally the system reaches a nonequilibrium steady state (NESS) and then determined the ensemble average quantities over many realizations of such trajectories. We show the correspondence between the evolution of the total and the medium entropy production with the average substrate binding and net velocity of the reaction in the context of detection of the cooperative behavior. Similarly this correspondence is also studied for the total entropy production rate at the NESS. The system entropy production is thoroughly studied in terms of the substrate binding probabilities for the different classes of cooperative systems considered. We have introduced a cooperativity index, C defined in terms of the stochastic system entropy to understand the nature of the cooperativity.

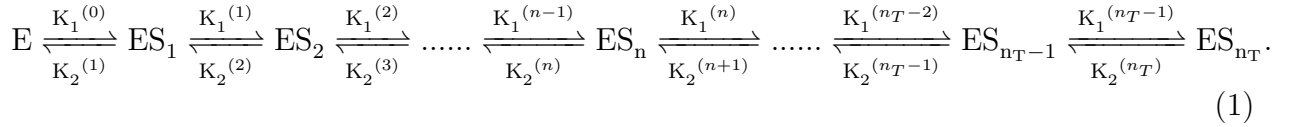
Layout of the paper is as follows. In Section II, we have given the master equations and their steady state solutions to describe the spatial and temporal cooperative binding mechanisms and the corresponding entropy production rates. In Section III, numerical results of entropy production and cooperative kinetics is discussed. In Section IV, we have discussed on measures of cooperativity and introduced an index of cooperativity. Then the paper is concluded in the Section V.

II. COOPERATIVE BINDING, MASTER EQUATION AND ENTROPY PRODUCTION RATE

In this section, we have first classified the cooperativity of a single oligomeric enzyme on the basis of the nature of the enzyme-substrate binding and then proposed a stochastic description for each class in terms of a one-dimensional random walk problem. Here we have provided a master equation approach for the description of spatial and temporal cooperativity which is suitable for the calculation of entropy production.

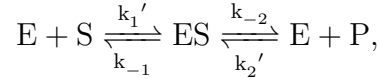
A. Classes of cooperativity: spatial and temporal substrate binding

Here we have considered that the substrate molecules can bind to the subunits of the oligomeric enzyme sequentially or independently as already discussed in the Introduction section. In the oligomeric enzyme kinetics reaction, the substrate molecules bind to the subunits of the oligomeric enzyme in a stepwise manner with different affinity which was first proposed by Adair to explain the cooperativity phenomenon observed in the oxygen-binding to the hemoglobin at equilibrium⁵¹. If an oligomeric enzyme consists of n_T number of homo or hetero type of subunits, then at the chemiostatic condition the substrate-binding scheme of the enzyme can be written as,



Here ES_n represents the conformational state of the oligomeric enzyme in which n number of subunits are occupied by the substrate molecules. $K_1^{(n-1)}$ and $K_2^{(n)}$ are designated as the total formation and total dissociation rate constants in the n -th reaction step, respectively.

The above scheme of substrate binding of an oligomeric enzyme can be viewed as a generalization of the kinetics of an enzyme having a single subunit given by



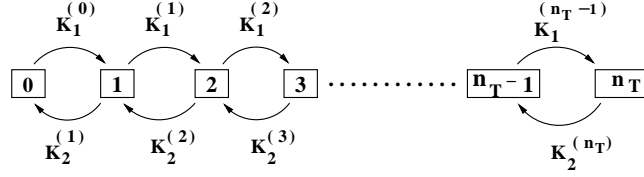
which can be further simplified as



Here $K_1 = (k_1 + k_2)$ and $K_2 = (k_{-1} + k_{-2})$, are designated as the total formation and total dissociation rate constants of ES , respectively. The pseudo first-order rate constants are written as $k_1 = k_1'[S]$ and $k_2 = k_2'[P]$ where $[S]$ and $[P]$ are the constant substrate and product concentration in the chemiostatic condition. Hence the site-dependent total formation and dissociation rate constants in the case of the oligomeric enzyme kinetics are similarly defined as $K_1^{(n-1)} = (k_1^{(n-1)} + k_2^{(n-1)})$ and $K_2^{(n)} = (k_{-1}^{(n)} + k_{-2}^{(n)})$ where $k_1^{(n-1)} = k_1'^{(n-1)}[S]$ and $k_2^{(n-1)} = k_2'^{(n-1)}[P]$.

The dynamics of the substrate binding mechanisms are quantified by counting the number of occupied sites present in the oligomeric enzyme at a particular instant of time. If at time t , 'n' number of occupied sites are present in the oligomeric enzyme (the state ES_n) then

a) Kinetic scheme of spatial cooperativity



b) Kinetic scheme of temporal cooperativity

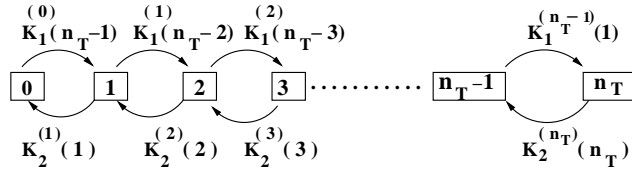


FIG. 1. Kinetic schemes for (a) spatial and (b) temporal cooperativity with site-dependent binding and dissociation rate constants. The numbers in the square boxes denote the number of occupied sites. In spatial cooperativity (a), the forward and backward transition probabilities depend only on the total formation and dissociation rate constants, respectively. For temporal cooperativity (b), the forward transition probability depends on the total formation rate constant and the number of unoccupied sites, whereas the backward transition probability depends on the total dissociation rate constant and the number of occupied sites.

at time $t + dt$, the number of occupied sites may be increased or decreased by one unit due to the occurrence of a formation or a dissociation reaction. During the time evolution, the number of occupied sites is a fluctuating quantity. Therefore, the system performs a one-dimensional random walk along the finite number of states where state- n of the system is equivalent to the conformational state ES_n , as shown in figure 1.

The kinetic scheme of the spatially cooperative system is given in figure 1(a). As the subunits get occupied sequentially starting from subunit-1, so when we say that the n -th subunit is occupied it automatically means that n number of sites are occupied in total. Here the forward and the backward transition probabilities depend only on the total formation and dissociation rate constants $K_1^{(n)}$ and $K_2^{(n)}$, respectively which are generally site-dependent.

This is so because after the filling of one subunit, there is no other choice for the next substrate molecule but to fill up the next adjacent subunit and as this is true for all the subunits, there is no combinatorial term in the transition probability.

The kinetic scheme for the temporal cooperativity is shown in figure 1(b). Here the substrate molecules can bind independently with any one of the n_T number of subunits. The state- n of the system represents n -number of occupied sites of the enzyme. In this mechanism, the forward transition probability of the n -th state at time t is given by the product of the total formation rate constant $K_1^{(n)}$ with the number of distinct combinations of unoccupied sites present at that time. Similarly, the backward transition probability of the same state is the product of the total dissociation rate constant, $K_2^{(n)}$ and the number of distinct combinations of occupied sites present at time t (see figure 1(b)). Here these rate constants are taken to be site-dependent in general. If all the rate constants are site-independent, then the system will be non-cooperative. The main difference of the sequential binding scheme from the independent one is as follows: *for the sequential scheme, the system will show spatial cooperativity in substrate binding even when the formation and dissociation rate constants are not site-dependent.*

B. Master equations

For the time-dependent description of the spatial cooperativity, we have constructed the corresponding master equation for this cooperativity mechanism as

$$\frac{\partial P_{\text{sp}}(n, t)}{\partial t} = K_1^{(n-1)} P_{\text{sp}}(n-1; t) + K_2^{(n+1)} P_{\text{sp}}(n+1; t) - (K_1^{(n)} + K_2^{(n)}) P_{\text{sp}}(n; t), \quad (3)$$

with $K_1^{(-1)} = K_2^{(0)} = K_1^{(n_T)} = K_2^{(n_T+1)} = 0$ to match the boundary terms. Here, $P_{\text{sp}}(n, t)$ is the probability of having n number of occupied sites at time t . We have given an analytical expression for the solution of the master equation by setting $\frac{\partial P_{\text{sp}}(n, t)}{\partial t} = 0$. The steady state distribution of the spatial cooperativity is given by

$$P_{\text{sp}}^{\text{SS}}(n) = \frac{\prod_{j=0}^{n-1} X^{(j)}}{\sum_{n=0}^{n_T} \prod_{j=0}^{n-1} X^{(j)}}, \quad (4)$$

where $X^{(j)} = \frac{K_1^{(j)}}{K_2^{(j+1)}} = \frac{k_1^{(j)}[S] + k_2^{(j)}}{k_{-1}^{(j+1)} + k_{-2}^{(j+1)}}$ with $j = 0, 1, \dots, (n_T - 1)$. Here the steady state is actually a nonequilibrium steady state (NESS) as already discussed. If $X^{(j)} = X \forall j$, the NESS

probability distribution becomes

$$P_{\text{sp}}^{\text{ss}}(\mathbf{n}) = \frac{X^n(1-X)}{1-X^{(n_T+1)}}, \quad (5)$$

which is a geometric distribution. The average population of the occupied sites at the NESS for $X^{(j)} = X \forall j$ is given by

$$\langle \mathbf{n} \rangle = \sum_{n=0}^{n_T} n P_{\text{sp}}^{\text{ss}}(\mathbf{n}) = \frac{X(1 - (n_T + 1)X^{n_T} + n_T X^{n_T+1})}{(1-X)(1-X^{n_T+1})}. \quad (6)$$

For temporal cooperativity, the master equation is written as

$$\begin{aligned} \frac{\partial P_{\text{temp}}(\mathbf{n}, t)}{\partial t} = & K_1^{(n-1)}(n_T - n + 1)P_{\text{temp}}(\mathbf{n} - 1; t) + K_2^{(n+1)}(n + 1)P_{\text{temp}}(\mathbf{n} + 1; t) \\ & - K_1^{(n)}(n_T - n)P_{\text{temp}}(\mathbf{n}; t) - K_2^{(n)}n P_{\text{temp}}(\mathbf{n}; t), \end{aligned} \quad (7)$$

again with $K_1^{(-1)} = K_2^{(0)} = K_1^{(n_T)} = K_2^{(n_T+1)} = 0$. Solving this master equation at the NESS, we can obtain the probability distribution as

$$P_{\text{temp}}^{\text{ss}}(\mathbf{n}) = \frac{\binom{n_T}{n} \prod_{j=0}^{n-1} X^{(j)}}{\sum_{n=0}^{n_T} \binom{n_T}{n} \prod_{j=0}^{n-1} X^{(j)}}, \quad (8)$$

where $X^{(j)} = \frac{K_1^{(j)}}{K_2^{(j+1)}}$ as already defined with $j = 0, 1, \dots, (n_T - 1)$. The average number of occupied sites at the NESS is simply expressed as

$$\langle \mathbf{n} \rangle = \frac{\sum_n n \binom{n_T}{n} \prod_{j=0}^{n-1} X^{(j)}}{\sum_{n=0}^{n_T} \binom{n_T}{n} \prod_{j=0}^{n-1} X^{(j)}}. \quad (9)$$

Now positive cooperativity in this scenario means a higher affinity of a second substrate molecule to attach with the oligomeric enzyme compared to that of the first substrate molecule which is already bound and so on. Therefore, in this case, the successive binding affinity of the substrate molecule increases. So naturally here we take the binding rate constants, $k_1^{(n)}$ as follows^{44,52}

$$k_1^{(0)} < k_1^{(1)} \dots < k_1^{(n)} < k_1^{(n+1)} < \dots < k_1^{(n_T-1)}. \quad (10)$$

Here the site-dependent overall association rate constant $K_1^{(n)}$ is defined as $K_1^{(n)} = k_1^{(n)} + k_2^{(n)}$ and similarly, the overall site-dependent dissociation rate constant is written as $K_2^{(n)} = k_{-1}^{(n)} + k_{-2}^{(n)}$. We take the rate constants $k_{-1}^{(n)}$, $k_2^{(n)}$ and $k_{-2}^{(n)}$ to be site-independent. This is due to the fact that to get a cooperative behavior for the independent binding case, it is not necessary to take all the rate constants of the reaction system to be site-dependent that will also make the results obtained hard to analyze. Then the site-dependent quantities $X^{(j)}$ for positive cooperativity maintain the relation:

$$X^{(0)} < X^{(1)} \dots < X^{(n)} < X^{(n+1)} < \dots < X^{(n_T-1)}. \quad (11)$$

Similarly, negative cooperativity arises as a second substrate molecule binds to the oligomeric enzyme with a lower affinity than that of the first substrate molecule. Therefore, the substrate binding reaction rate constants for different sites obey the inequalities

$$k_1^{(0)} > k_1^{(1)} \dots > k_1^{(n)} > k_1^{(n+1)} > \dots > k_1^{(n_T-1)}. \quad (12)$$

Then taking the rate constants $k_{-1}^{(n)}$, $k_2^{(n)}$ and $k_{-2}^{(n)}$ as site-independent constants, we have

$$X^{(0)} > X^{(1)} \dots > X^{(n)} > X^{(n+1)} > \dots > X^{(n_T-1)}. \quad (13)$$

If all the association and dissociation rate constants are site-independent, then the enzyme becomes non-cooperative. Thus the steady state distribution, Eq.(8) reduces to

$$P^{ss}(\mathbf{n}) = \binom{n_T}{n} \frac{X^n}{(1+X)^{n_T}}, \quad (14)$$

where $X = \frac{K_1}{K_2}$. By inserting the value of X , the above equation can be written as a binomial distribution given by

$$P^{ss}(\mathbf{n}) = \binom{n_T}{n} \left(\frac{K_1}{K_1 + K_2} \right)^n \left(\frac{K_2}{K_1 + K_2} \right)^{(n_T-n)} = P^{(bino)}(\mathbf{n}). \quad (15)$$

This is expected, as in the absence of any cooperativity, the distribution of the occupied sites must follow a binomial distribution. So for a system with no cooperativity, the average number of occupied sites at the NESS is

$$\langle \mathbf{n} \rangle = n_T \left(\frac{X}{1+X} \right) = n_T \left(\frac{K_1}{K_1 + K_2} \right) \quad (16)$$

and the average number of unoccupied sites is

$$\langle n_T - n \rangle = n_T \left(\frac{K_2}{K_1 + K_2} \right). \quad (17)$$

We mention that, in addition to the overall association and dissociation rate constants being site-independent, if the rate constant k_2 is also negligibly small, then the enzyme kinetics becomes simply the Michaelis-Menten type. If $k_2^{(j)}$ ($j = 0, \dots, (n_T - 1)$) is taken to be much less than the other rate constants, then we have

$$X^{(j)} = \frac{[S]}{K_M^{(j)}}, \quad (18)$$

where $K_M^{(j)} = \frac{k_{-1}^{(j+1)} + k_{-2}^{(j+1)}}{k_1^{(j)}}$ can be described as the stepwise Michaelis-Menten constant.

C. Entropy production rates

The system entropy is defined in terms of the Shannon entropy as

$$S_{\text{sys}}(t) = -k_B \sum_n P(n, t) \ln P(n, t), \quad (19)$$

where $P(n, t)$ is the probability of having n number of occupied states at time t with $P(n, t) \equiv P_{\text{sp}}(n, t)$ or $P(n, t) \equiv P_{\text{temp}}(n, t)$. Here we set the Boltzmann constant, $k_B = 1$. Using the master equation, one can get the system entropy production rate⁵³⁻⁵⁶ as

$$\begin{aligned} \dot{S}_{\text{sys}}(t) &= \frac{1}{2} \sum_{n, \mu} [w_{\mu}(n - \nu_{\mu}|n)P(n - \nu_{\mu}, t) - w_{-\mu}(n|n - \nu_{\mu})P(n, t)] \\ &\quad \times \ln \frac{P(n - \nu_{\mu}, t)}{P(n, t)}. \end{aligned} \quad (20)$$

Here the state of the system can change by any one of the four reactions, denoted with index μ , via which the substrate and the product molecules can bind with the enzyme sites and detach. They are given as: (1) $(ES_n + S) \xrightarrow{k_1^{(n)}} (ES_{n+1})$ ($\mu = 1$), (2) $(ES_n) \xrightarrow{k_{-1}^{(n)}} (ES_{n-1} + S)$ ($\mu = -1$), (3) $(ES_n) \xrightarrow{k_{-2}^{(n)}} (ES_{n-1} + P)$ ($\mu = -2$) and (4) $(ES_n + P) \xrightarrow{k_2^{(n)}} (ES_{n+1})$ ($\mu = 2$). Here ν_{μ} is designated as the stoichiometric coefficient of the μ -th reaction with rate constant k_{μ} where $\nu_{\mu} = 1$ with $\mu > 0$ and $-\nu_{\mu} = 1$ with $\mu < 0$. The transition probabilities are defined as follows

$$w_{\mu}(n - \nu_{\mu}|n) = k_{\mu}^{(n - \nu_{\mu})} (n_T - (n - \nu_{\mu})), \mu > 0$$

and

$$w_\mu(n - \nu_\mu | n) = k_\mu^{(n - \nu_\mu)}(n - \nu_\mu), \mu < 0. \quad (21)$$

We have assumed ideal reservoir(surroundings) with no inherent entropy production except through the boundaries of the system. The system entropy production rate(epr) can be split as⁵⁵

$$\dot{S}_{\text{sys}}(t) = \dot{S}_{\text{tot}}(t) - \dot{S}_{\text{m}}(t). \quad (22)$$

Here the first term in the r.h.s. of equation(22) gives the total entropy production rate and the second term denotes the medium entropy production rate due to the entropy flux into the surroundings. Therefore the total and medium entropy production rates are defined as

$$\begin{aligned} \dot{S}_{\text{tot}}(t) &= \frac{1}{2} \sum_{n, \mu} [w_\mu(n - \nu_\mu | n)P(n - \nu_\mu, t) - w_{-\mu}(n | n - \nu_\mu)P(n, t)] \\ &\quad \times \ln \frac{w_\mu(n - \nu_\mu | n)P(n - \nu_\mu, t)}{w_{-\mu}(n | n - \nu_\mu)P(n, t)} \end{aligned} \quad (23)$$

and

$$\begin{aligned} \dot{S}_{\text{m}}(t) &= \frac{1}{2} \sum_{n, \mu} [w_\mu(n - \nu_\mu | n)P(n - \nu_\mu, t) - w_{-\mu}(n | n - \nu_\mu)P(n, t)] \\ &\quad \times \ln \frac{w_\mu(n - \nu_\mu | n)}{w_{-\mu}(n | n - \nu_\mu)}. \end{aligned} \quad (24)$$

At steady state, $\dot{S}_{\text{sys}} = 0$ (whether equilibrium or NESS). An NESS is characterized by a non-zero total epr given by

$$\begin{aligned} \dot{S}_{\text{tot}}^{(\text{NESS})} &= \sum_n [w_1(n - 1 | n)P(n - 1) - w_{-1}(n | n - 1)P(n)] \\ &\quad \times \ln \left(\frac{w_1(n - 1 | n)P(n - 1) \times w_{-2}(n | n - 1)P(n)}{w_{-1}(n | n - 1)P(n) \times w_2(n - 1 | n)P(n - 1)} \right). \end{aligned} \quad (25)$$

This equation is derived using the circular balance condition⁵⁷

$$\begin{aligned} w_1(n - 1 | n)P(n - 1) - w_{-1}(n | n - 1)P(n) &= \\ w_{-2}(n | n - 1)P(n) - w_2(n - 1 | n)P(n - 1). \end{aligned} \quad (26)$$

Now here we consider two limiting situations.

(i) It is clear that if we do not consider the presence of the product species then there will be just two sets of rate constants, $k_1^{(n)}$ and $k_{-1}^{(n)}$. Then at the steady state, the balance condition that holds is obviously the detailed balance which gives

$$w_1(n - 1 | n)P(n - 1) - w_{-1}(n | n - 1)P(n) = 0.$$

Then from Eq.(25), we have $\dot{S}_{\text{tot}} = 0$ at the steady state which is reduced now to an equilibrium. Now from Eq.(18), the quantity $X^{(j)}$ under this condition becomes $X^{(j)} = \frac{k_1^{(j)}[S]}{k_{-1}^{(j+1)}}$ where $\frac{k_1^{(j)}}{k_{-1}^{(j+1)}}$ are the stepwise equilibrium (binding) constants. So in this limit, theoretically there is no difference between our model and a protein-ligand binding model which generally does not consider the product formation.

(ii) Another interesting point is that if we consider the case where $k_1^{(n)}, k_{-1}^{(n)} \gg k_{-2}^{(n)}$ (with $k_2^{(n)}$ being already considered negligible) then this corresponds to the pre-equilibrium limit or simply the equilibrium limit. The assumption is valid when fast reversible reactions precede slower reactions in a reaction network. Now in this situation also, the quantity $X^{(j)}$ is defined in terms of the stepwise equilibrium (binding) constants. In this context, we mention that the original derivation of the enzyme catalysis reaction by Michaelis and Menten involved the pre-equilibrium assumption with the equilibrium dissociation constant parameter. The more general derivation by Briggs and Haldane used the steady state approximation and their expression contained the actual Michaelis-Menten constant. In our case also we see the same features in the quantity, $X^{(j)}$ which is the parameter of our model study. In the general nonequilibrium case, $X^{(j)}$ is related to the stepwise Michaelis-Menten constant, $K_M^{(j)}$ (see Eq.(18) with $k_2^{(j)}$ considered negligible) whereas in the absence of product species leading to equilibrium or under the pre-equilibrium assumption, $X^{(j)}$ is related to the stepwise equilibrium (binding) constant, $\frac{k_1^{(j)}}{k_{-1}^{(j+1)}}$.

III. NUMERICAL SIMULATION OF ENTROPY PRODUCTION

In this section, we have calculated the medium, system and the total entropy production for the spatial and temporal cooperative systems. For a given initial condition, the oligomeric enzyme system reaches NESS at a particular time which depends on the chemio-static condition, *i.e.*, the value of the constant substrate concentration. The initial condition is taken as the fully unbound state of the enzyme with all the subunits being vacant *i.e.*, $P(n, t = 0) = \delta_{n,0}$. This condition leads to zero system entropy at $t=0$. For the time-dependent system entropy production calculation in general, one needs the time-dependent solution of the master equation, $P(n, t)$. But here the final time in the calculation of the entropy production over the time interval (starting at $t = 0$ with the specified initial condition above) is taken such that by then the system reaches the NESS and hence steady

state solutions are all we need to get the system entropy production over the length of the trajectory. The total entropy production for a single trajectory is calculated over the time interval where the determination of the medium entropy production requires the detailed information of the path and not just the initial and final points. We run the simulations in all the cases up to a fixed point of time taken to be the same for all the binding mechanisms. As the steady state is an NESS (and not an equilibrium), total and medium entropy production increase linearly with time and hence if the final point of time is not the same for all the cases, one can not compare the various entropy production values for the different cooperative systems.

A. Implementation of the scheme of single trajectory stochastic simulation

Along a single stochastic trajectory the system entropy production can be defined as²¹ $\mathbf{S}(\mathbf{t}) = -\ln p(\mathbf{n}, \mathbf{t})$, where $p(\mathbf{n}, \mathbf{t})$ is the solution of the stochastic master equation for a given initial condition, $p(\mathbf{n}_0, t_0)$, taken along the specific trajectory $\mathbf{n}(\mathbf{t})$. Note that, the single trajectory entropy is denoted by (bold) \mathbf{S} whereas the trajectory-average entropy production (equivalent to ensemble average) is denoted by S . Now at the microscopic level, the number of occupied sites of the oligomeric enzyme becomes a fluctuating quantity due to the random occurrence of the different reaction events within the random time interval. This develops the concept of different trajectories. Here the state of the system can change by any one of the four reactions (denoted with index μ) as discussed in Sec.IIC.

A stochastic trajectory, $\mathbf{n}(\mathbf{t})$ starting at the state \mathbf{n}_0 , jumping at times t_j from the state \mathbf{n}_{j-1} to the state \mathbf{n}_j and finally ending up at \mathbf{n}_l with $t = t_l$ is defined as,

$$\mathbf{n}(\mathbf{t}) \equiv (\mathbf{n}_0, t_0) \xrightarrow{\nu_\mu^{(1)}} (\mathbf{n}_1, t_1) \xrightarrow{\nu_\mu^{(2)}} \dots \rightarrow (\mathbf{n}_{j-1}, t_{j-1}) \xrightarrow{\nu_\mu^{(j)}} (\mathbf{n}_j, t_j) \rightarrow \dots \rightarrow (\mathbf{n}_{l-1}, t_{l-1}) \xrightarrow{\nu_\mu^{(l)}} (\mathbf{n}_l, t_l). \quad (27)$$

Here $\mathbf{n}_j = \mathbf{n}_{j-1} + \nu_\mu^{(j)}$ where $\nu_\mu^{(j)}$ is the stoichiometric coefficient of the μ -th reaction along a trajectory and $t_j = t_{j-1} + \tau_j$ where τ_j is the time interval between two successive jumps. During the jump from the $(\mathbf{n}_j - 1)$ state to the \mathbf{n}_j state, any one of the four reactions will occur (see Eq. (1) and Eq. (2)). The rate constant of the reaction μ is denoted as k_μ . The time interval τ_j between the two jumps is a random variable following the exponential distribution^{49,50}

$$p(\tau_j) = a \exp(-a\tau_j) \quad (28)$$

with $a = \sum_{\mu=\pm 1}^{\pm 2} w(\mathbf{n}_j - 1; \nu_\mu^j)$. Here $w(\mathbf{n}_{j-1}; \nu_\mu^j)$ denotes the forward transition probability

from the state $(n_j - 1)$ to the state n_j through a reaction channel μ with the stoichiometric coefficient $\nu_\mu^{(j)}$.

Now a time reversed trajectory can be defined as,

$$\mathbf{n}^R(t) \equiv (n_1, t_1) \xrightarrow{-\nu_\mu^{(1)}} (n_{1-1}, t_{1-1}) \xrightarrow{-\nu_\mu^{(1-1)}} \dots \rightarrow (n_j, t_j) \xrightarrow{-\nu_\mu^{(j)}} (n_{j-1}, t_{j-1}) \dots \rightarrow (n_1, t_1) \xrightarrow{-\nu_\mu^{(1)}} (n_0, t_0). \quad (29)$$

This time reversed trajectory is generated due to the occurrence of a reaction channel whose state changing vector $-\nu_\mu^{(j)}$ is exactly opposite to the state changing vector $\nu_\mu^{(j)}$ of the forward reaction channel.

The time-dependent total entropy production, $\Delta \mathbf{S}_{\text{tot}}$ along a trajectory can be split into a system part, $\Delta \mathbf{S}_{\text{sys}}$ and a medium contribution, $\Delta \mathbf{S}_{\text{m}}$. Hence the change of total entropy along a trajectory can be written as²¹

$$\Delta \mathbf{S}_{\text{tot}} = \Delta \mathbf{S}_{\text{m}} + \Delta \mathbf{S}_{\text{sys}} \quad (30)$$

where

$$\Delta \mathbf{S}_{\text{sys}} = \ln \frac{p(n_0, t_0)}{p(n, t)} \quad (31)$$

and

$$\Delta \mathbf{S}_{\text{m}} = \sum_j \ln \frac{w(n_{j-1}; \nu_\mu^{(j)})}{w(n_j; -\nu_\mu^{(j)})}. \quad (32)$$

Here $w(n_{j-1}; \nu_\mu^{(j)})$ denotes the forward transition probability as already defined. Similarly, $w(n_j; -\nu_\mu^{(j)})$ denotes the backward transition probability from the state n_j to the $(n_j - 1)$ state through a reaction channel μ with the exactly opposite stoichiometric coefficient $-\nu_\mu^{(j)}$.

B. Cooperative kinetics

To simulate the spatial cooperativity associated with the sequential binding, we have taken the site-independent reaction rate constants as $k'_1 = 0.015 \mu\text{M}^{-1}\text{s}^{-1}$ and $k_{-1} = 7.0$, $k_{-2} = 2.0$, $k_2 = 0.001$, all in s^{-1} . The substrate concentration is taken in μM unit. The total number of subunits present in the oligomeric enzyme is taken as $n_T = 3$. We have calculated the various entropy productions using the stochastic simulation for single trajectories over a time interval starting from the initial condition to a final time as mentioned above. We have taken 2×10^5 trajectories to get the ensemble average of the entropy production values. We have calculated the average binding number, $\langle n \rangle$ for this case from Eq.(6) and the net product

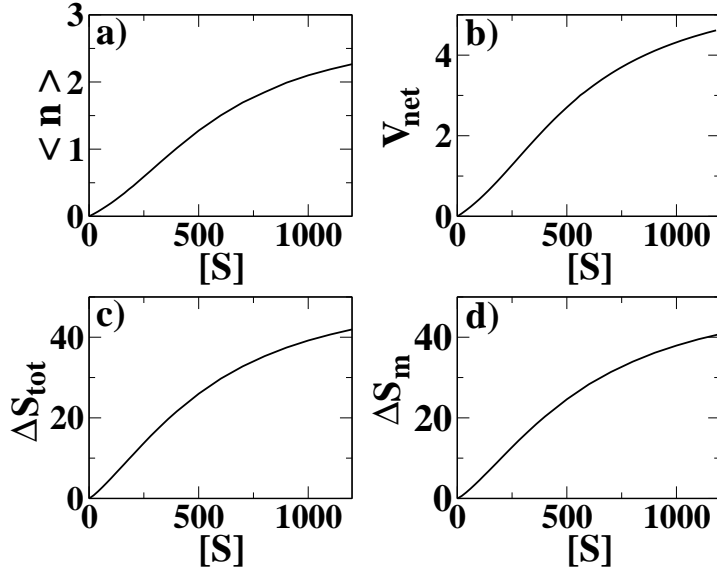


FIG. 2. (a) $\langle n \rangle$ and (b) v_{net} for the spatial cooperative (sequential) binding as a function of substrate concentration, $[S]$ (in μM unit) at the NESS. (c) and (d) exhibit the corresponding ΔS_{tot} and ΔS_{m} variations with $[S]$. The entropy productions are calculated over a time interval that starts with the given initial condition (see text) and ends with the system at the NESS.

formation rate by using the formula, $v_{\text{net}} = k_{-2}\langle n \rangle - k_2\langle n_{\text{T}} - n \rangle$, at the final time where the system resides at the NESS. We have plotted these quantities as a function of the substrate concentration in figure 2(a) and (b). It is clear from the plots that both the quantities grow with a sigmoidal shape as a function of substrate concentration indicating positive cooperativity in substrate binding. According to Eq.(6), this is due to the higher power (> 1) dependence of $\langle n \rangle$ on the factor X which is proportional to the substrate concentration. As the rate constants are taken as site-independent, the positive cooperativity generated in the system is inherent in the binding mechanism. Now we have plotted ΔS_{tot} and ΔS_{m} , both being ensemble averages taken over the 2×10^5 realizations of the trajectories, in figure 2(c) and (d), respectively, against the substrate concentration. Interestingly, we find the nature of both the curves to be sigmoidal.

Next we come to the case of independent substrate binding that can give rise to the case of temporal cooperativity with site-dependent reaction rate constants. To simulate the entropy production for the positive cooperative system, we take the rate constants of successive substrate binding steps as (see Eq.(10)): $k_1^{(1)} = f^{(1)}k_1^{(0)}$ and $k_1^{(2)} = f^{(2)}k_1^{(0)}$, where $k_1^{(0)} = k_1^{\prime(0)}[S]$ with $k_1^{\prime(0)} = 0.015 \mu\text{M}^{-1}\text{s}^{-1}$. The set $\{k_1^{\prime(0)}, k_{-1}, k_{-2}, k_2\}$ is called the starting

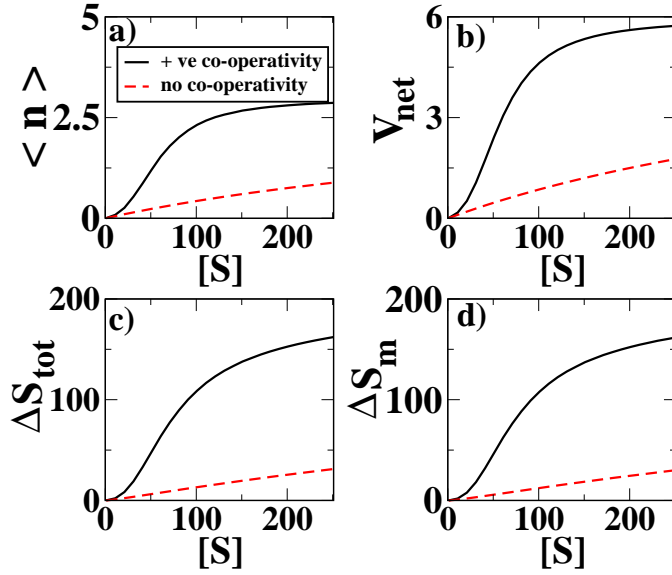


FIG. 3. (a) $\langle n \rangle$ and (b) v_{net} for the temporally cooperative (independent) binding with positive cooperativity against substrate concentration, $[S]$ (in μM unit) at the NESS. (c) and (d) give the corresponding ΔS_{tot} and ΔS_{m} variations with $[S]$. The entropy productions are calculated over a time interval as described in the caption of figure 2. It is evident from the figure that all the curves show a significant sigmoidal behavior indicating the positive cooperativity.

or initial rate constants of the cooperative system. For the simulation, here we take $f^{(1)} = 10$ and $f^{(2)} = 100$, *i.e.*, a 10-fold increase in substrate binding rate constants in each step. The other rate constants are site-independent and taken to be the same as in the case of the spatial cooperativity. We also calculate the average binding number using Eq.(9) and the net product formation rate, at the NESS. They are shown in figure 3 (a) and (b) along with the total and the medium entropy production in figure 3(c) and (d), respectively, all as a function of the substrate concentration. It is evident from the figure that all the curves show a significant sigmoidal behavior indicating the positive cooperativity. We have also given the corresponding quantities in the case of non-cooperativity in the same plot for comparison. The non-cooperative case is simulated with site-independent rate constants same as in the case of the spatial cooperativity. In this case $\langle n \rangle$ is determined using Eq.(16). We see that in this case also, the nature of variation of $\langle n \rangle$, v_{net} , ΔS_{m} and ΔS_{tot} with the substrate concentration is the same, hyperbolic to be specific.

Now we come to the last case in this category, *i.e.*, the negative cooperativity. In this case,

the rate constants of the substrate binding reaction are taken as (see Eq.(12)): $k_1^{(0)} = 1.5 \mu\text{M}^{-1}\text{s}^{-1}$, $k_1^{(1)} = f^{(1)}k_1^{(0)}$ and $k_1^{(2)} = f^{(2)}k_1^{(0)}$ with the values of the factors being $f^{(1)} = 0.1$ and $f^{(2)} = 0.01$, *i.e.*, a 10-fold decrease in substrate binding rate constant in each step. The other rate constants are taken as in the previous cases. The value of $k_1^{\prime(0)}$ is taken to be 100 times greater compared to the cases of spatial and positive cooperativity. This is only for the demonstration of the negative cooperativity effect on the binding curves of the reaction. We have plotted $\langle n \rangle$ against substrate concentration in figure 4(a) for the negative as well as the non-cooperative case. Here for the non-cooperative case also we have taken $k_1^{\prime(0)} = 1.5 \mu\text{M}^{-1}\text{s}^{-1}$. Both the curves show the hyperbolic nature. The two cases are distinguished by plotting $\frac{1}{\langle n \rangle}$ versus $\frac{1}{[S]}$ which is the Lineweaver-Burk plot. For non-cooperative enzyme, this plot gives a straight line whereas the curve for the negative cooperative binding starts at a higher value on the y-axis and becomes nonlinear when it comes close to the curve of the non-cooperative system at high substrate concentration. This feature is shown in figure 4(b). Now we have plotted similar curves for ΔS_{tot} in figure 4(c) and (d). One can see the same hyperbolic nature in the plot of ΔS_{tot} versus substrate concentration (figure 4(c)) for both the cases and the nonlinearity in the plot of $\frac{1}{\Delta S_{\text{tot}}}$ versus $\frac{1}{[S]}$ at high substrate concentration for the negative cooperativity (figure 4(d)). So from the above discussion and the plots, we conclude that the familiar indications of the cooperative behavior in substrate binding, given in terms of the nature of variation of the average binding number and the net velocity of the reaction as a function of the substrate concentration, are all reflected in the same manner in the corresponding variation of the total as well as the medium entropy production.

We have also calculated the total entropy production rate, \dot{S}_{tot} at the NESS using Eq.(25) for all the cases of cooperativity. Here we have taken the same set of rate constants as we have already considered to calculate the various entropy productions. The variations of \dot{S}_{tot} with substrate concentration, $[S]$ for different binding schemes are shown in figure 5. It is evident from the figure that the features of cooperative binding are also reflected in a similar fashion on the variation of \dot{S}_{tot} with substrate concentration.

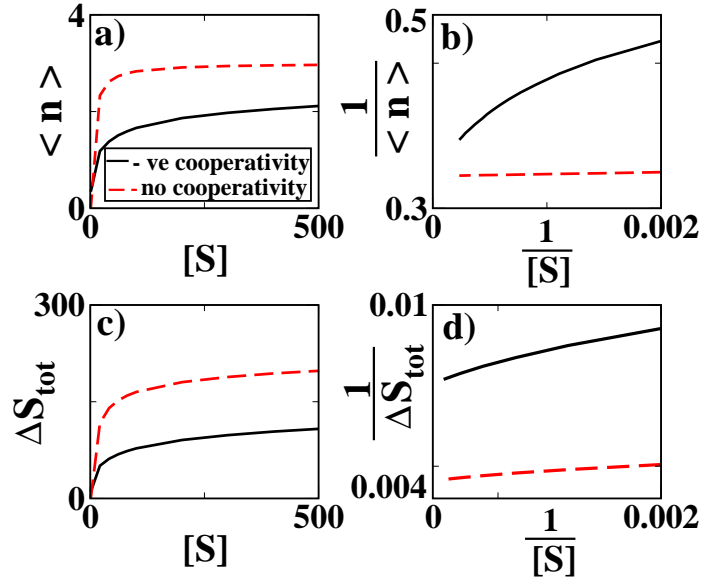


FIG. 4. Plots of (a) $\langle n \rangle$ vs. $[S]$ (in μM unit) and (b) $\frac{1}{\langle n \rangle}$ vs. $\frac{1}{[S]}$ at the NESS. (c) ΔS_{tot} vs. $[S]$ and (d) $\frac{1}{\Delta S_{\text{tot}}}$ versus $\frac{1}{[S]}$ for negative cooperative (temporal) as well as non-cooperative binding. The entropy productions are calculated over a time interval as described in the caption of figure 2.

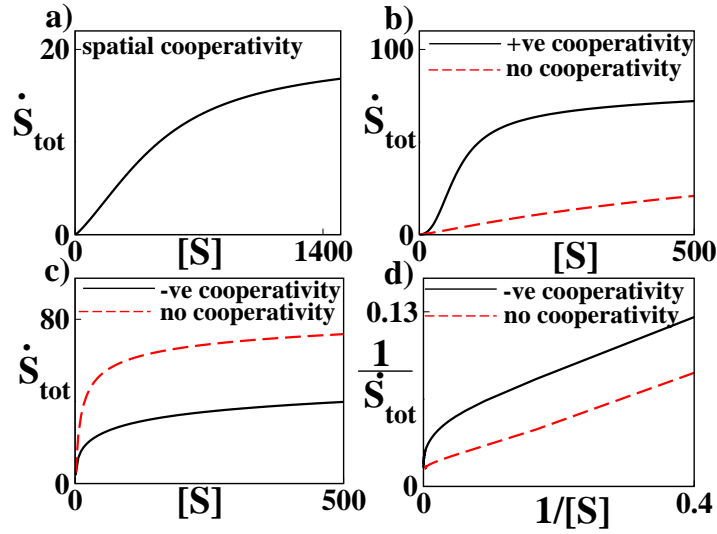


FIG. 5. (a) Plot of \dot{S}_{tot} against substrate concentration, $[S]$ (in μM unit) for spatial cooperativity. In (b) and (c), the same quantity is plotted for positive and negative cooperative cases, respectively. The non-cooperative case is also shown for comparison. (d) Plot of $\frac{1}{\dot{S}_{\text{tot}}}$ vs. $\frac{1}{[S]}$, which is a Lineweaver-Burk type plot, for negative and non-cooperative cases.

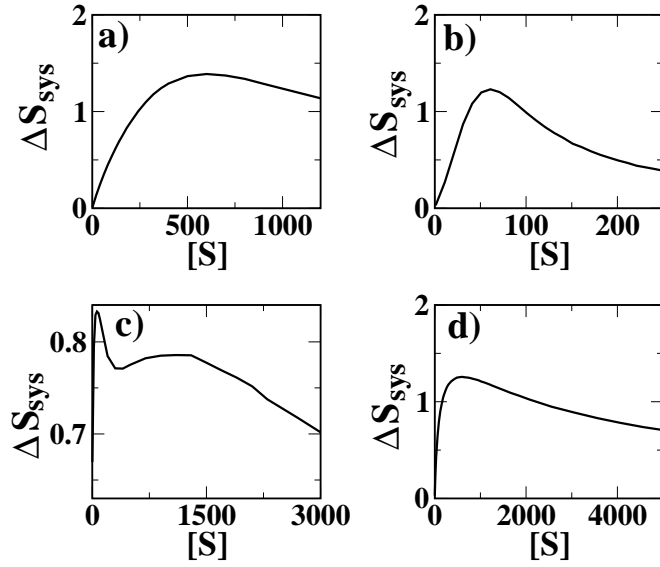


FIG. 6. Plot of ΔS_{sys} against substrate concentration, $[S]$ (in μM unit) for (a) spatial cooperative binding, (b) positive (temporal) cooperative binding, (c) negative (temporal) cooperative binding and (d) non-cooperative binding. In all the cases, the final time of observation is the same, set as such that the system reaches the NESS.

C. System entropy production and binding characteristics

The ensemble or trajectory average system entropy production over the time interval can be written as

$$\Delta S_{\text{sys}} = S_{\text{sys}}^{\text{final}} - S_{\text{sys}}^{\text{initial}} = - \sum_{n=0}^{n_T} P^{\text{ss}}(n) \ln P^{\text{ss}}(n), \quad (33)$$

where the initial condition (time $t = 0$) of the fully unbound enzyme gives $S_{\text{sys}}^{\text{initial}} = 0$ and the final state of the system is an NESS characterized by the distribution $P^{\text{ss}}(n)$. We have plotted the ensemble average system entropy production, ΔS_{sys} as a function of the substrate concentration in figure 6 for all the cases. In figure 6(a), ΔS_{sys} is plotted for spatial cooperativity and in figure 6(b-d) it is shown for the positive, negative and non-cooperative cases, respectively which belong to the class of temporal cooperativity. The first thing evident from the plots is that ΔS_{sys} passes through a global maximum for all the cases and in the case of negative cooperativity, there is also a local maximum with the parameters of our system.

We have plotted $P^{\text{ss}}(n)$ as a function of the substrate concentration in figure 7(a-d) with

the steady state ('ss') superscript being dropped for simplicity. Figure 7(a) shows the curves for spatial cooperativity. We can see that they all cross almost exactly at the same point, $[S] \sim 600 \mu\text{M}$ giving rise to the maximum in ΔS_{sys} for spatial cooperativity at this point (see figure 6(a)). In figure 7(b), we have shown the curves for the positively cooperative system. At $[S] \sim 60 \mu\text{M}$, the curves cross in a pairwise fashion; curves of $P(0)$ and $P(3)$ cross each other at this point as well as curves for $P(1)$ and $P(2)$. This particular substrate concentration corresponds to the maximum of ΔS_{sys} in this case (see figure 6(b)).

The case of negative cooperativity requires a bit more attention. There is again pairwise curve crossing of the two sets of probabilities same as in the case of positive cooperativity at the same substrate concentration shown in figure 7(c). This gives rise to the global maximum in the curve of ΔS_{sys} for this type of binding shown in figure 6(c). The local maximum can be explained as follows. Unlike the plots in figure 7(a) and (b), the probability curves $P(2)$ and $P(3)$ remain at significant values over the substrate range studied and the dominance of these two probability curves in figure 7(c) (actually when $P(2)$ and $P(3)$ cross, they are close to 0.5 at $[S] \sim 1800 \mu\text{M}$) over a large substrate range gives rise to an increase of ΔS_{sys} , albeit slow. Finally we come to the case of non-cooperativity in figure 7(d) where again there is the pairwise crossing of the same set of probabilities as in figure 7(b) but at $[S] \sim 600 \mu\text{M}$ that again gives rise to the maximum of ΔS_{sys} shown in figure 6(d). In this case too, there are more than one dominating probability curves before and after the pairwise crossing over similar substrate range as in figure 7(c). But the ΔS_{sys} in this case shows a slow but steady decrease with substrate concentration after passing through the maximum without any unusual behavior. This may be due to the fact that here at least three of the four probabilities are significant (with comparable values) over a large substrate range and so they do not cross the value of 0.5 in this range unlike the case in figure 7(c). It is clear that arbitrary variation of the rate constants of the system in each binding step can make life more complicated and then the maxima in the ΔS_{sys} curve may or may not be associated with the binding probability curve crossings.

We can justify the curve crossings, whether they all cross or cross pairwise at a particular substrate concentration, by inspecting the expressions of the steady state probability distributions. We see from the steady state distribution for the spatial cooperativity, Eq.(5), that if one of the probabilities, say $P(0)$ is approximately equal to any other probability, say $P(3)$, then $X \sim 1$ (but obviously not exactly equal to 1) and this automatically leads to the

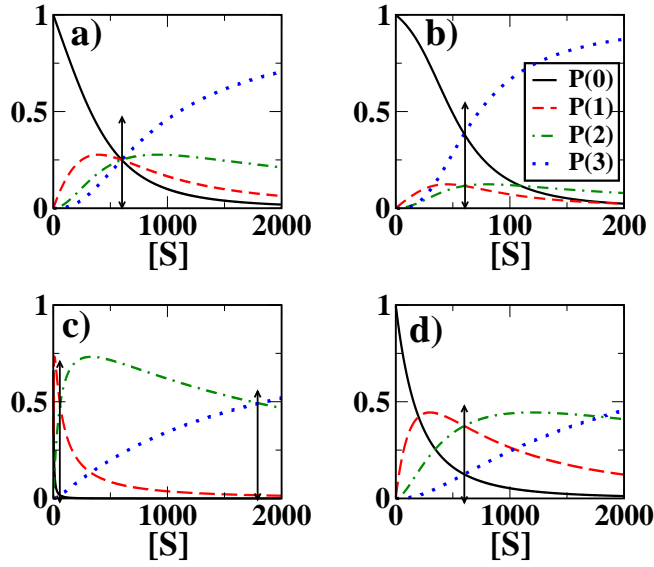


FIG. 7. Plot of the steady state distributions, $P^{\text{ss}}(n)$ against $[S]$ (in μM unit) for (a) spatial cooperative binding, (b) positive (temporal) cooperative binding, (c) negative (temporal) cooperative binding and (d) non-cooperative binding. In the plots, the ‘ss’ superscript is dropped for simplicity. The arrows indicate the curve crossing points.

near equality of all the probabilities at this value of X . This is true for all the probabilities and hence in this case the probabilities can only cross simultaneously at $X \sim 1$. As the probabilities are equal at this point which corresponds to $[S] \sim 600 \mu\text{M}$, this obviously gives the maximum system entropy production in this case. Now we take the steady state distribution of the non-cooperative case, Eq.(14). It can be easily seen that here only $P(0) = P(3)$ leads to the equality $P(1) = P(2)$ at $X = 1$ giving the maximum of ΔS_{sys} again at $[S] \sim 600 \mu\text{M}$. So in the context of the system entropy production the spatial cooperative system shows some similarity with the non-cooperative system. With the same set of site-independent rate constants, the spatial cooperative system is also associated with larger system entropy production compared to that of the non-cooperative case. This is because all the binding probabilities become equal for the spatial cooperativity whereas they become equal pairwise for non-cooperative binding.

The cases of positive and negative cooperativity belonging to the class of temporal cooperativity are a bit complicated. We have considered a 10-fold increase of the substrate binding rate constant for each successive binding in the case of positive cooperativity whereas a 10-fold decrease in the corresponding rate constant for each successive binding for negative

cooperativity. This symmetry ensures that in both the cases only $P(0) = P(3)$ leads to the equality $P(1) = P(2)$ at $X^{(1)} = 1$. This can be easily proved from Eq.(8). But if the rise or fall of the value of the substrate binding rate constant in each successive step of binding is not by the same factor, then the pairwise equality of the binding probabilities is not possible at a given substrate concentration.

IV. MEASURE OF COOPERATIVITY

Here we have discussed on the determination of the Hill coefficient from the master equation corresponding to the different binding schemes. We have also introduced an index of cooperativity in terms of the stochastic system entropy associated with the fully bound state of the cooperative and non-cooperative cases. We have analyzed its connection to the Hill coefficient using some relevant experimental data which gives a realistic application of the proposed scheme of measurement of cooperativity.

A. Hill coefficient

In the traditional enzymology, the characterization of cooperativity is carried out by measuring the Hill coefficient³³. For positive and negative cooperative cases, the Hill coefficient becomes greater than or less than one, respectively, whereas the non-cooperative case is characterized with Hill coefficient equal to one. Experimentally it is obtained by determining the fractional saturation, $\theta(= \langle n \rangle / n_T)$ at various substrate concentrations $[S]$, constructing the Hill plot ($\ln(\frac{\theta}{1-\theta})$ vs. $\ln[S]$) and then finding the slope at the half-saturation point, $\theta = 0.5$ or at a point where the slope deviates maximum from unity. On the other hand, Hill coefficient is theoretically defined as the ratio of the variances of the binding number of the cooperative and non-cooperative cases at the half-saturation point with the non-cooperative binding case following the binomial distribution^{39,58}.

We briefly mention the features of the Hill plot for the model binding schemes studied here. The slope of the Hill plot is generally given by³⁹

$$H = \frac{[S](d\theta/d[S])}{\theta(1-\theta)}. \tag{34}$$

For temporal cooperativity, the fractional saturation can be written as (see Eq.(9))

$$\theta_{\text{temp}} = \frac{\sum_n n B_n [S]^n}{n_T \sum_n B_n [S]^n}, \quad (35)$$

where $B_n = \binom{n_T}{n} \prod_{j=0}^{n-1} (K_M^{(j)})^{-1}$ with $B_0 = 1$. Then one gets

$$H_{\text{temp}} = \frac{\langle n^2 \rangle - \langle n \rangle^2}{n_T \theta (1 - \theta)} = \frac{\sigma_{\text{temp}}^2}{\sigma_{\text{bino}}^2}, \quad (36)$$

where σ_{temp}^2 and σ_{bino}^2 are the variances of the binding numbers of the temporal and non-cooperative cases, respectively. The Hill coefficient, n_H is given at the half-saturation point as³⁹ $n_H = \frac{4\sigma_{\text{temp}}^2}{n_T}$. Similar expressions hold for the spatial cooperative binding. We have already mentioned in Sec.IIB that if all the rate constants of the independent binding scheme are site-independent, then the binding is non-cooperative with binomial distribution of the binding probability. Here we discuss the corresponding scenario for the sequential binding (leading to spatial cooperativity) to be non-cooperative in terms of the variance of the binding number. In the case of spatial cooperativity, the variance of the binding number, σ_{sp}^2 is given by

$$\sigma_{\text{sp}}^2 = \left(\frac{1+X}{1-X} \right) \langle n \rangle - \langle n \rangle^2 - \frac{n_T (n_T + 1) X^{n_T+1}}{1 - X^{n_T+1}}, \quad (37)$$

where X and $\langle n \rangle$ are as given in Eq.(5) and Eq.(6). Now for $n_T = 1$, this reduces to

$$\sigma_{\text{sp}}^2 = \frac{X}{(1+X)^2} = \sigma_{\text{bino}}^2. \quad (38)$$

and then the slope of the Hill plot becomes $H_{\text{sp}} = \frac{\sigma_{\text{sp}}^2}{\sigma_{\text{bino}}^2} = 1$ for any substrate concentration. So for sequential binding, the cooperative behavior is absent only if the enzyme is monomeric.

B. Cooperativity index

Here we introduce an index of cooperativity. First we build up the concept from binding probabilities and then demonstrate how this index can indicate the nature of the cooperativity. For positive cooperative binding, one expects that full occupancy of the enzyme is more probable compared to the case of non-cooperativity. Similarly, for negative cooperativity, the full occupancy of the enzyme is less probable. Now, if the probability of an event- n is p_n , then the associated surprisal is given by $-\ln(p_n)$ and more probable the event, the less is its surprisal. So the ratio of the surprisals, associated with the probability of the system to

remain in a fully occupied state without and with cooperativity at NESS, should be greater than 1 for positive cooperativity and less than 1 for negative cooperativity. Hence we define the index of cooperativity, denoted by C in terms of the ratio of the surprisals, associated with the probability of the system to remain in a fully occupied state without and with cooperativity at NESS as

$$C = \frac{-\ln(P^{(\text{bino})}(n_T))}{-\ln(Q(n_T))} \quad (39)$$

where the binomial distribution, $P^{(\text{bino})}$ is the reference corresponding to the non-cooperative case and the distribution Q corresponds to the cooperative binding case. The rate constants of the reference non-cooperative system (binomial) must be the same as those of the starting or initial rate constants of the cooperative system for the comparison to be valid. The relation is then independent of the actual value of the (constant) substrate concentration. We point out that the surprisal is equivalent to the single trajectory stochastic system entropy^{21,59} (associated with the fully occupied state). So the index, C is truly an entropic estimate of cooperativity at the microscopic level.

Based on the above argument, next we theoretically analyze the probability to remain in a fully occupied state for different cooperative systems and compare that with the non-cooperative case to formulate the criteria of cooperativity in terms of C . For spatial cooperativity, the ratio of its steady state distribution (Eq.(5)) and the reference binomial distribution (Eq.(14)) for $n = n_T$ is given by

$$R_{\text{sp}} = \frac{P_{\text{sp}}^{\text{ss}}(n_T)}{P^{(\text{bino})}(n_T)} \\ = 1 + \frac{\left[\left(\binom{n_T}{1} - \binom{n_T}{0} \right) X + \left(\binom{n_T}{2} - \binom{n_T}{1} \right) X^2 + \dots + \left(\binom{n_T}{n_T} - \binom{n_T}{n_T-1} \right) X^{n_T} \right]}{(1 - X^{n_T+1})}. \quad (40)$$

From the above expression it is clear that for all values of X , either greater than or less than 1, the quantity R_{sp} is greater than 1 indicating positive cooperativity. This will lead to the condition $C > 1$ for the case of spatial cooperativity for any substrate concentration. Only in the case of monomeric enzyme, ($n_T = 1$), the system will be non-cooperative with $R_{\text{sp}} = C = 1$ as already discussed in terms of variances at the end of Sec.IVA.

In the case of temporal cooperativity, the corresponding ratio, R_{temp} is given using Eq.(8) and Eq.(14) at $n = n_T$ as

$$R_{\text{temp}} = \frac{P_{\text{temp}}^{\text{ss}}(n_T)}{P^{(\text{bino})}(n_T)}$$

$$\begin{aligned}
&= \left[\frac{\frac{X^{(0)}X^{(1)}\dots X^{(n_T-1)}}{[1+n_T X^{(0)}+\dots+(X^{(0)}X^{(1)}\dots X^{(n_T-1)})]}}{\frac{X^{n_T}}{(1+X)^{n_T}}} \right] \\
&= \left[\frac{\frac{(X^{(0)})^{n_T} f^{(n_T-1)}}{[1+n_T X^{(0)}+\dots+(X^{(0)})^{n_T} f^{(n_T-1)}]}}{\frac{(X^{(0)})^{n_T}}{[1+n_T X^{(0)}+\dots+(X^{(0)})^{n_T}]}}, \right. \tag{41}
\end{aligned}$$

with $X^{(0)} = X$. Now both $P_{\text{temp}}^{\text{ss}}(n_T)$ and $P^{(\text{bino})}(n_T)$ tend to 1 at large $X^{(0)}$ *i.e.* large substrate concentration. But it is clear that for positive cooperative binding with $f > 1$, the last term in the denominator of $P_{\text{temp}}^{\text{ss}}(n_T)$ dominates the previous terms more readily compared to the case of $P^{(\text{bino})}(n_T)$. Hence at a particular substrate concentration, $P_{\text{temp}}^{\text{ss}}(n_T)$ is closer to 1 compared to $P^{(\text{bino})}(n_T)$ and so R_{temp} is greater than 1. For negative cooperativity with $f < 1$, the situation is obviously reverse and R_{temp} is less than 1. Therefore, in the light of the above discussions and Eq.(39), we write down the condition of cooperativity in terms of C as

$$C \begin{cases} > 1, \text{ positive cooperativity} \\ = 1, \text{ no cooperativity} \\ < 1, \text{ negative cooperativity.} \end{cases} \tag{42}$$

This is the same criteria of cooperativity as given in terms of the Hill coefficient. To find out the Hill coefficient, *i.e.*, the variances theoretically, it is necessary to know the probability distribution of the corresponding positive and negative cooperativity cases, respectively. Now our measure of cooperativity, the index C, is also related to the probability distributions; but it is defined in terms of the ratio of a specific term of the distributions, namely the probability of the fully occupied state. So apparently there is no straightforward connection between the Hill coefficient and C. The Hill coefficient is the slope of the binding curve at a particular substrate concentration corresponding to the half-saturation point whereas the index C is defined independent of the substrate concentration and the characterization of cooperativity in terms of C is valid at any substrate concentration.

We have plotted the quantity, C in figure (8) for positive cooperative system (independent binding) and also for the spatial cooperative binding for different values of n_T as a function of substrate concentration. For the positive cooperativity case, the substrate binding rate constants, $k_1^{(n)}$ increase by a factor of 2 in each step. The value of C grows with substrate concentration, starting just above 1.0 and finally saturates. One can see from Eq.(39), that the limiting value of C (obtained at high substrate concentration) in case of spatial cooperativity is n_T whereas for temporal cooperativity it is given by $f^{(n_T-1)}$ where $f^{(n_T-1)} =$

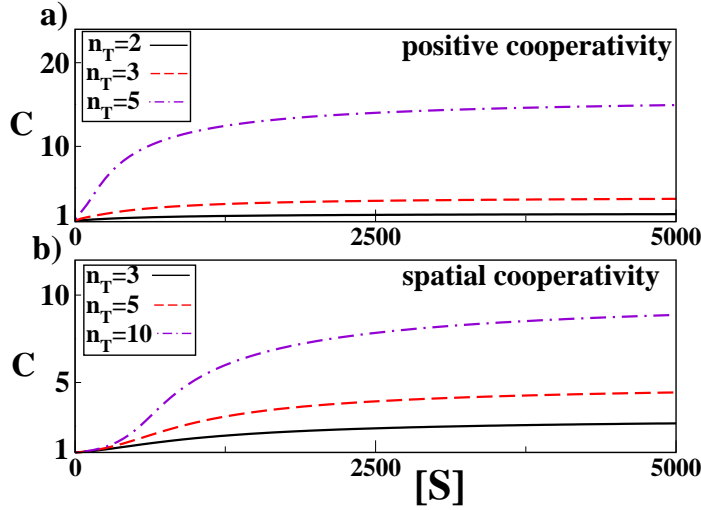


FIG. 8. Plot of the cooperativity index, C against substrate concentration, $[S]$ (in μM unit) for different values of the number of subunits of the oligomeric enzyme, n_T in the case of (a) positive (temporal) cooperativity and (b) spatial cooperativity.

$\frac{k_1^{(n_T-1)}}{k_1^{(0)}}$. These results are discussed in detail in the appendix. Here we specifically mention the case of $n_T = 5$ for the positive cooperativity where the limiting value of C is $f^{(4)} = \frac{k_1^{(4)}}{k_1^{(0)}} = 2^4 = 16$. It is evident from figure (8)(a) that this is indeed the case.

C. Characterization of cooperativity: a case study with stepwise Aspartate receptor binding

Although apparently there is no straightforward connection between the Hill coefficient, n_H and C , first of all it is clear that the well-known criteria of cooperativity in terms of n_H is exactly the criteria we have given in terms of the cooperativity index, C in Eq.(42). Both the measures are equal to 1 in the absence of cooperativity whereas for cooperative binding, the criteria are the same although the actual values of n_H and C will be generally different. Here we will try to illustrate this point using some experimental data from the work of Kolodziej *et al.*⁵² regarding the production of positive, negative as well as non-cooperativity by mutations at a serine 68 residue located at the subunit interface in the dimeric aspartate receptor of *Salmonella typhimurium*. Due to unavailability of experimental data of the

stepwise Michaelis-Menten constants, $K_M^{(j)}$, we use the stepwise binding constants reported in their study in the place of $(K_M^{(j)})^{-1}$ of the independent binding model with $n_T = 2$ and $j = 0, 1$. Now the parameter $X^{(j)}$ in our study is related to $K_M^{(j)}$ in the general non-equilibrium condition and reduces to stepwise equilibrium (binding) constants under the conditions already discussed at the end of Sec.IIC. For experimental testability of C at NESS, one needs the stepwise Michaelis-Menten constants, $K_M^{(j)}$. We choose the independent binding model as the experimental result reports both positive and negative cooperativity. We calculate the fractional saturation θ as a function of substrate concentration, $[S]$ using Eq.(9) and find out the Hill coefficient, n_H at the half-saturation point ($\theta = 0.5$). Then we determine the cooperativity index, C at the substrate concentration where $\theta = 0.5$. The results are given in Table. 1. The Hill coefficients derived by us for different cases tally very well with the experimental data⁵². The cooperativity index, C detects the presence and absence of cooperativity successfully. Also the extent or degree of positive or negative cooperative behavior is equally well characterized by the index, C. This can be seen by comparing the values of n_H and C for the cases of serine and cysteine showing negative cooperativity as well as for threonine and isoleucine showing positive cooperativity.

TABLE I. The stepwise Aspartate binding constants, K'_1 and K'_2 (in μM^{-1}) for different amino acid residues at position 68 of Aspartate receptor taken from the experimental study of Kolodziej *et al*⁵². Here we have taken the values of the inverse of the stepwise Michaelis-Menten constants, $K_M^{(j)}$ in our model to be equal to the binding constants. The values of the Hill coefficient, n_H in the parentheses are from the experimental work, given for comparison with the values determined here. The cooperativity index, C characterizes the cooperative behavior successfully as can be seen by comparing it with n_H .

Amino acid	$\frac{1}{K_M^{(0)}} (= K'_1)$	$\frac{1}{K_M^{(1)}} (= K'_2)$	n_H	C
serine	0.7	0.2	0.7(0.7)	0.491
cysteine	0.5	0.2	0.776(0.8)	0.598
threonine	0.4	0.9	1.197(1.2)	1.519
isoleucine	0.4	2.8	1.446(1.4)	2.558
aspartate	0.1	0.1	1.0(1.0)	1.0

The cooperativity index, C is related to the probability of fully bound state of the single

enzyme. So another possibility of experimentally determining C , apart from the measurement of the stepwise Michaelis-Menten constants, will be to detect this fully bound state by electrical or optical means in a single molecule experiment and then to fit the resulting probability with some model distribution.

V. CONCLUSION

We have classified the cooperative substrate binding phenomena of a single oligomeric enzyme on the basis of the binding mechanism and the nature of the substrate-bound states of the system in a chemiostatic condition. Both the binding mechanisms are modelled in terms of master equation. The sequential binding of the substrate molecules leads to spatial cooperativity whereas the independent binding scheme leads to temporal cooperativity. We have determined the various entropy productions due to the enzyme kinetics over a time interval where at the final point of time the system is in a nonequilibrium steady state (NESS) that can be arbitrarily far away from equilibrium. We have used kinetic Monte Carlo simulation algorithm applied on a single trajectory basis to calculate the entropy production. In this context, the interesting finding is that the total as well as the medium entropy production show the same diagnostic signatures for detecting the cooperativity as is well known in terms of the average binding number or the net velocity of the reaction. More specifically, ΔS_{tot} as well as ΔS_{m} for positive cooperative kinetics show sigmoidal variation as a function of substrate concentration whether the class being spatial or temporal. They also show the non-linearity in the inverse plot of Lineweaver-Burk type demonstrating the case of negative cooperativity. The signs of cooperative behavior is also reflected in a similar fashion on the variation of the total entropy production rate (epr) with substrate concentration determined at the NESS for different binding schemes. That the features of cooperativity are reflected similarly on the variations of both the total epr at the NESS and the total (and medium) entropy production over a time interval up to the NESS is a highly interesting fact and gives deep insight on the role of the binding mechanism in governing the total entropy production in a general non-equilibrium setup.

We have thoroughly analyzed the system entropy production for all the cases in terms of the steady state binding probability distributions. For a spatial and a non-cooperative system, the maximum value of the system entropy production due to the nonequilibrium

processes in the reaction appears at the same substrate concentration with the value of the entropy production being greater for the spatial cooperativity. We have explained this in terms of the different binding probability curve-crossings that helps to understand how the binding characteristics affect the entropy production of the system, *i.e.*, the single oligomeric enzyme. Similarly, the distinct features of the evolution of system entropy production for the positive and negative cooperative binding give valuable insights on its connection to the binding mechanism.

We have introduced an index of cooperativity, C defined as the ratio of the surprisal or equivalently, the stochastic system entropy associated with the fully bound state of the cooperative and non-cooperative cases. The criteria of cooperativity in terms of C is identical to that of the Hill coefficient. We have analyzed its connection to the Hill coefficient using some relevant experimental data. This index is truly an entropic estimate of cooperativity and gives a microscopic insight on the cooperative binding of substrate on a single oligomeric enzyme instead of realising cooperativity in terms of macroscopic reaction rate.

Acknowledgement : K.B. acknowledges the Council of Scientific and Industrial Research (C.S.I.R.), India for the partial financial support as a Senior Research Fellow.

Appendix: Estimate of the limiting value of the cooperativity index, C for various cooperative binding

Here the limiting value of the cooperativity index, C for the spatial and temporal cooperative binding are determined at high substrate concentration. The limiting value of the cooperativity index, C for the spatial cooperativity is calculated from Eq.(39) by using the steady state probability distribution function of spatial cooperativity, $P_{sp}^{ss}(n)$ (Eq.(5)) and that of no cooperativity, $P_{bino}^{ss}(n)$ (Eq.(14)) at $n = n_T$. The expression of C then becomes

$$C = \frac{-\ln \left[\left(\frac{X}{1+X} \right)^{n_T} \right]}{-\ln \left[\frac{X^{n_T}(1-X)}{1-X^{(n_T+1)}} \right]}. \quad (\text{A.1})$$

At high substrate concentration, with $X \gg 1$, the above equation can be written as

$$C = \frac{n_T \ln \left(1 + \frac{1}{X} \right)}{-\ln \left(1 - \frac{1}{X} \right)}. \quad (\text{A.2})$$

Now expanding the log terms in the Eq. (A.2) and neglecting the higher order terms, we

finally obtain

$$C = n_T. \quad (\text{A.3})$$

Therefore, the limiting value of C in the case of spatial cooperativity, obtained at high substrate concentration, is equal to the total number of sub-units of the oligomeric enzyme.

In a similar fashion, the limiting value of C can be calculated for the temporal cooperativity from Eq.(39) by using the steady state probability distribution function of temporal cooperativity, $P_{\text{temp}}^{\text{ss}}(n)$ (Eq.(8)) and that of no cooperativity, $P_{\text{bino}}^{\text{ss}}(n)$ (Eq.(14)) at $n = n_T$. At this value the distribution, $P_{\text{temp}}^{\text{ss}}(n)$ can be written as

$$P_{\text{temp}}^{\text{ss}}(n_T) = \frac{X^{(0)}X^{(1)}\dots X^{(n_T-1)}}{[1 + n_T X^{(0)} + \dots + (X^{(0)}X^{(1)}\dots X^{(n_T-1)})]}. \quad (\text{A.4})$$

Here $X^{(j)} \approx f^{(j)}X^{(0)}$ with $j = 0, \dots, (n_T - 1)$. This follows from the definition of $X^{(j)}$ (see Eq.(8) and Eq.(4)) with the small value of k_{-2} taken in this study. Now at high substrate concentration with $X^{(0)} \gg 1$, the above equation can be written as

$$P_{\text{temp}}^{\text{ss}}(n_T) = \frac{1}{[1 + \frac{n_T}{X^{(0)}f^{(n_T-1)}}]}. \quad (\text{A.5})$$

Now, by using the value of $P_{\text{temp}}^{\text{ss}}(n_T)$ and $P_{\text{bino}}^{\text{ss}}(n_T)$ into the Eq.(39) at high substrate concentration, we obtain

$$C = \frac{n_T \ln(1 + \frac{1}{X})}{\ln[1 + \frac{n_T}{X^{(0)}f^{(n_T-1)}}]}. \quad (\text{A.6})$$

For the comparative study of the temporal and non-cooperative cases, the starting value, $X^{(0)}$ is taken equal to X . Then expanding the log terms in the above equation and neglecting the higher order terms, we finally obtain the limiting value of C for temporal cooperativity as

$$C = f^{(n_T-1)} = \frac{k_1^{(n_T-1)}}{k_1^{(0)}}. \quad (\text{A.7})$$

Here we mention that for the negative cooperative binding, $f^{(n_T-1)}$ can be much less than 1 in general. But here we consider the case $X^{(0)}f^{(n_T-1)} \gg 1$.

REFERENCES

REFERENCES

- ¹D. Collin, F. Ritort, C. Jarzynski, S. B. Smith, I. Tinoco Jr., and C. Bustamante, *Nature*, **437**, 231 (2005).

- ²C. Jarzynski, *Nature Phys.*, **7**, 591 (2011).
- ³J. Liphardt, S. Dumont, S. B. Smith, I. Tinoco. Jr., and C. Bustamante, *Science*, **296**, 1832 (2002).
- ⁴H. Wang, and G. Oster, *Nature*, **396**, 279 (1998).
- ⁵D. M. Carberry, M. A. B. Baker, G. M. Wang, E. M. Sevick, and D. J. Evans, *J. Opt. A: Pure Appl. Opt.*, **9**, S204 (2007).
- ⁶F. Ritort, C. Bustamante, and I. Tinoco Jr., *Proc. Natl. Acad. Sci. USA*, **99**, 13544 (2002).
- ⁷C. Bustamante, J. Liphardt, and F. Ritort, *Physics Today*, **58**, 43 (2005).
- ⁸A. Mossa, S. De Lorenzo, J. M. Hugueta, and F. Ritort, *J. Chem. Phys.*, **130**, 234116 (2009).
- ⁹M. Manosas, A. Mossa, N. Forns, J. M. Hugueta, and F. Ritort, *J. Stat. Mech.*, P02061 (2009).
- ¹⁰F. Ritort, *Adv. Chem. Phys.*, **137**, 31 (2008).
- ¹¹T. Schmiedl, T. Speck, and U. Seifert, *J. Stat. Phys.*, **128**, 77 (2007).
- ¹²U. Seifert, *Europhys. Lett.*, **70** (1), 36 (2005).
- ¹³D. J. Evans, E. G. D. Cohen, and G. P. Morriss, *Phys. Rev. Lett.*, **71**, 2401 (1993).
- ¹⁴G. Gallavotti, and E. G. D. Cohen, *Phys. Rev. Lett.*, **74**, 2694 (1995).
- ¹⁵J. L. Lebowitz, and H. Spohn, *J. Stat. Phys.*, **95**, 333 (1999).
- ¹⁶G. E. Crooks, *Phys. Rev. E*, **60**, 2721 (1999).
- ¹⁷T. Hatano, and S. I. Sasa, *Phys. Rev. Lett.*, **86**, 3463 (2001).
- ¹⁸G. Gallavotti, *Phys. Rev. Lett.*, **77**, 4334 (1996).
- ¹⁹C. Jarzynski, *Phys. Rev. Lett.*, **78**, 2690 (1997).
- ²⁰E. M. Sevick, R. Prabhakar, S. R. Williams, and D. J. Searles, *Annu. Rev. Phys. Chem.*, **59**, 603 (2008).
- ²¹U. Seifert, *Phys. Rev. Lett.*, **95**, 040602 (2005).
- ²²T. Schmiedl, and U. Seifert, *J. Chem. Phys.*, **126**, 044101 (2007).
- ²³V. Blickle, T. Speck, L. Helden, U. Seifert, and C. Bechinger, *Phys. Rev. Lett.*, **96**, 070603 (2006).
- ²⁴C. Tietz, S. Schuler, T. Speck, U. Seifert, and J. Wrachtrup, *Phys. Rev. Lett.*, **97**, 050602 (2006).
- ²⁵H. Qian, and E. L. Elson, *Biophys. Chem.*, **101**, 565 (2002).
- ²⁶W. Min, L. Jiang, J. Yu, S. C. Kou, H. Qian, and X. S. Xie, *Nano Lett.*, **5**, 2373 (2005).

- ²⁷H. Qian, *Annu. Rev. Phys. Chem.*, **58**, 113 (2007).
- ²⁸B. Das, and G. Gangopadhyay, *J. Chem. Phys.*, **132**, 135102 (2010).
- ²⁹H. P. Lu, L. Xun, and X. S. Xie, *Science*, **282**, 1877 (1998).
- ³⁰S. C. Kou, B. J. Cherayil, W. Min, B. P. English, and X. S. Xie, *J. Phys. Chem B*, **109**, 19068, (2005).
- ³¹H. Ge, and M. Qian, *J. Chem. Phys.*, **129**, 015104 (2008).
- ³²H. Qian, *Biophys. J.*, **95**, 10 (2008).
- ³³T. Palmer, and P. Bonner, *Enzymes: Biochemistry, Biotechnology, and Clinical Chemistry*, 2nd ed., (Horwood Publishing, West Sussex, 2007).
- ³⁴J. Ricard, and A. Cornish-Bowden, *Eur. J. Biochem.*, **166**, 255 (1987).
- ³⁵G. G. Hammes, and C. W. Wu, *Annu. Rev. Biophys. Bioeng.*, **3**, 1 (1974).
- ³⁶A. Goldbeter, *Biophys. Chem.*, **4**, 159 (1976).
- ³⁷G. Weber, and S. R. Anderson, *Biochemistry*, **4**, 1942 (1965).
- ³⁸A. Levitzki, and D. E. Koshland Jr., *Proc. Natl. Acad. Sci. USA*, **62**, 1121 (1969).
- ³⁹H. Abeliovich, *Biophys. J.*, **89**, 76 (2005).
- ⁴⁰H. Qian, and J. A. Cooper, *Biochemistry*, **47**, 2211 (2008).
- ⁴¹A. Cornish, and A. L. Cardenas, *J. Theor. Biol.*, **124**, 1 (1987).
- ⁴²C. Frieden, *Annu. Rev. Biochem.*, **48**, 471 (1979).
- ⁴³K. E. Neet, and G. R. Ainslie, *Methods Enzymol.*, **64**, 192 (1980).
- ⁴⁴J. N. Weiss, *FASEB J.*, **11**, 835 (1997).
- ⁴⁵D. C. Gadsby, R. F. Rakowski, and P. Deweer, *Science*, **260**, 100 (1993).
- ⁴⁶J. Monod, J. Wyman, and J. P. Changeux, *J. Mol. Biol.*, **12**, 88 (1965).
- ⁴⁷D. E. Koshland Jr., G. Nemethy, and D. Filmer, *Biochemistry*, **5**, 365 (1966).
- ⁴⁸N. Bindslev, *Drug-acceptor interactions: modeling theoretical tools to test and evaluate experimental equilibrium effects*, 1st ed. (Co-Action Publishing, Sweden, 2008).
- ⁴⁹D. T. Gillespie, *J. Comput. Phys.*, **22**, 403 (1976).
- ⁵⁰D. T. Gillespie, *J. Phys. Chem.*, **81**, 2340 (1977).
- ⁵¹G. S. Adair, *J. Biol. Chem.*, **63**, 529 (1925).
- ⁵²A. F. Kolodziej, T. Tan, and D. E. Koshland Jr., *Biochemistry*, **35**, 14782 (1996).
- ⁵³D. Andrieux, and P. Gaspard, *J. Chem. Phys.*, **121**, 6167 (2004).
- ⁵⁴P. Gaspard, *J. Chem. Phys.*, **120**, 8898 (2004).
- ⁵⁵L. Jiu-li, C. Van den Broeck, and G. Nicolis, *Z. Phys. B*, **56**, 165 (1984).

- ⁵⁶G. Nicolis, and I. Prigogine, *Self-Organization in nonequilibrium Systems* (Wiley, New York, 1977).
- ⁵⁷M. Vellela, and H. Qian, *J. R. Soc. Interface*, **6**, 925 (2009).
- ⁵⁸J. J. Wyman, *Adv. Protein Chem.*, 19, 223 (1964).
- ⁵⁹M. Esposito, and C. Van den Broeck, *Phys. Rev. E*, **82**, 011143 (2010).